# EVALUATING AXIAL DRILLED SHAFT RESPONSE BY SEISMIC CONE

Paul W. Mayne[1], M.ASCE and James A. Schneider[2], Assoc. M.ASCE

*Foundations & Ground Improvement*, GSP 113, ASCE, Reston/VA, pp. 655-669.

**Abstract**

The axial load-displacement-capacity of drilled shaft foundations can be conveniently evaluated using the results of seismic piezocone penetration tests (SCPTU) to provide continuous profiles of small- and large-strain soil properties. The penetration readings ($q_T$, $f_s$, and $u_b$) reflect soil limit states that are utilized to obtain the side and base components for capacity, while the initial soil-pile stiffness is assessed from measurements of downhole shear wave velocity ($V_s$) via elastic continuum theory. An equivalent elastic modulus coupled with degradation scheme provides nonlinear representation with increasing load level. Load transfer from top to base is considered and the approach can accommodate homogeneous to generalized Gibson-type soil conditions. A recent load test case study is presented for a drilled shaft situated in Piedmont residuum for an interstate highway bridge in Coweta County, GA.

## Introduction

The evaluation of drilled shaft foundations for support of large axial loads from buildings, towers, and bridges is usually separated into two analysis procedures: (1) axial capacity, and (2) axial displacements at working loads. In the calculations of capacity, different methods are available depending upon whether the loading is undrained or drained, the soils are fine-grained or granular or intermediate geomaterials, as well as the applied direction of loading (compression vs. uplift). For analyses involving displacements, methods are available based on spring models or subgrade reaction (t-z curves), elastic continuum theory, and empirical relationships. Details on these approaches are succinctly summarized by O'Neill and Reese (1999).

[1] Professor, School of Civil & Environmental Engineering, Georgia Institute of Technology, Atlanta, GA 30332-0355; Phone: 404-894-6226; Email: pmayne@ce.gatech.edu
[2]Project Geotechnical Engineer, Fugro West Inc., 4820 McGrath Street, Suite 100,Ventura, CA 93003-7778 Email: JSchneider@fugro.com

In reality, the axial response of deep foundations changes progressively from small

strains that occur elastically at initial stress states (corresponding to the nondestructive region and $K_0$ conditions) and develop to elastic-plastic states corresponding to intermediate strains, eventually reaching plastic failure (as well as post-peak) conditions. Numerical approximations using finite elements, discrete elements, finite differences, and boundary elements can be used to follow the stress paths at points near, intermediate, and far away from the soil-pile interfaces. However, simplified analytical methods also have merit in that quick and reliable assessments can be made using spreadsheets or programmable calculators.

With the recent interest in cone penetration testing for geotechnical site characterization, it is timely to discuss the use of seismic piezocone testing for the evaluation of both axial capacity (obtained from the penetration data) and initial stiffness ($E_0$) for use in deformation response, especially since the test provides data at opposite ends of the stress-strain-strength response of soils, as illustrated by Figure 1 (Burns & Mayne, 1996). A modified hyperbola (Fahey & Carter, 1993) can be used to conveniently degrade the initial stiffness with increasing load level and provide nonlinear load-displacement-capacity results.

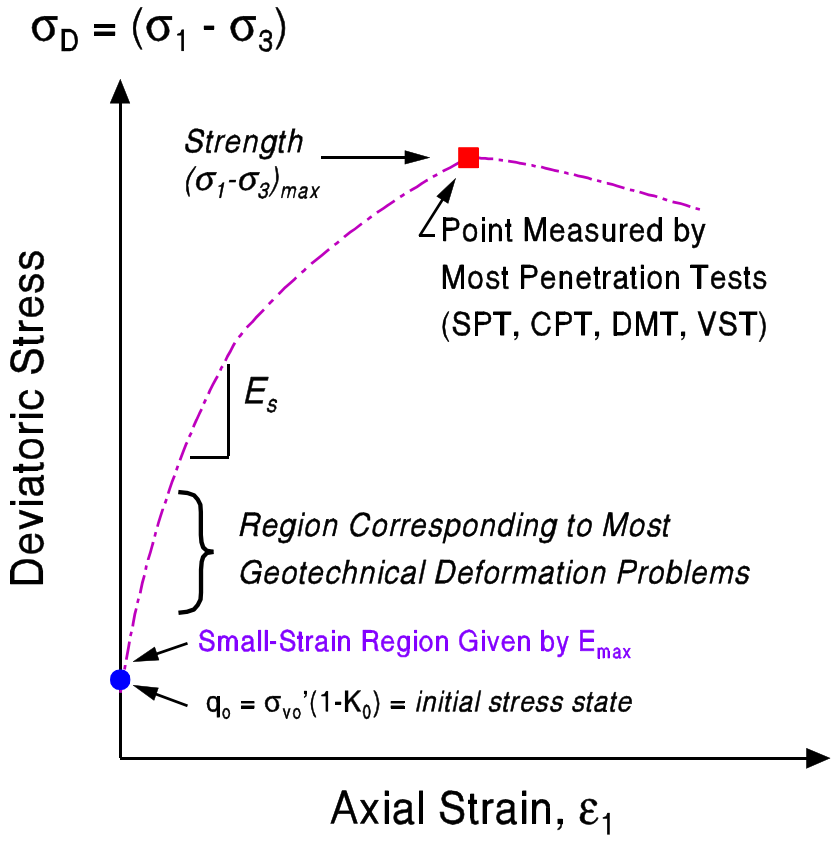


**Figure 1.**
**Stresses and Stiffnesses of Soils at Small- and Large-Strains**

**Small-Strain Modulus**

Recent research outside of the U.S. has found that the small-strain stiffness from shear wave velocity ($V_s$) measurements applies to the initial static monotonic loading, as well as the dynamic loading of geomaterials (Burland, 1989; Tatsuoka & Shibuya, 1992; LoPresti et al., 1993). Thus, the original dynamic shear modulus ($G_{dyn}$) has been re-termed the maximum shear modulus, designated $G_{max}$ or $G_0$, that provides an upper limit stiffness given by: $G_0 = \rho_T V_s^2$ where $\rho_T$ = total mass density of the soil. This is a fundamental stiffness of all solids in civil engineering and can be measured in all soil types from colloids, clays, silts, sands, gravels, to boulders and fractured rocks. The corresponding equivalent elastic modulus is found from: $E_0 = 2G_0 (1+\nu)$ where $\nu = 0.2$ is the approximate value of Poisson's ratio of geomaterials at small strains.

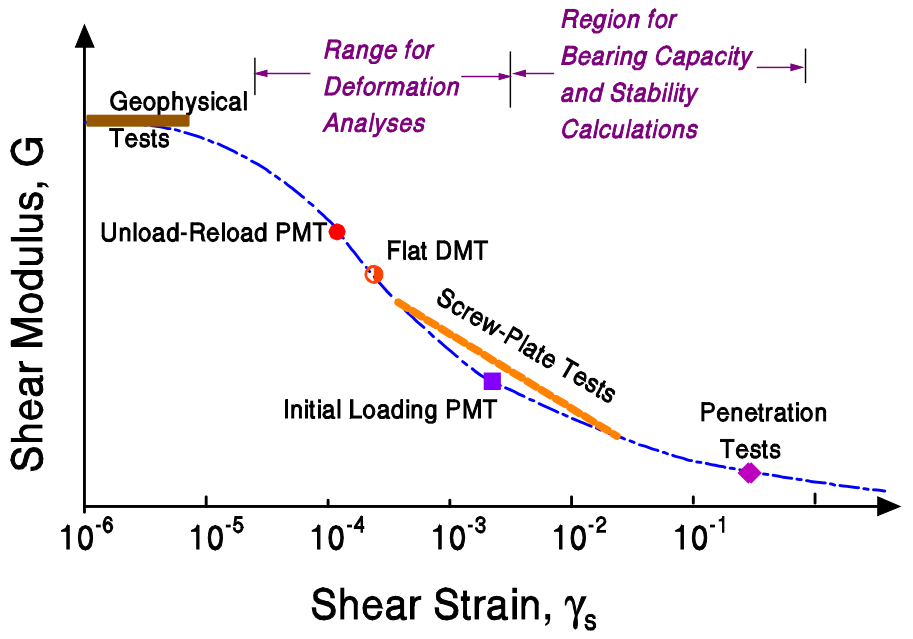


**Figure 2. Variation of Shear Modulus with Strain Level and Relevance to In-Situ Tests.**

The stress-strain-strength-time response of soils is complex, highly nonlinear, and depends upon loading direction, anisotropy, rate effects, stress level, strain history, time effects, and other factors. It is therefore a difficult issue to recommend a single test, or even a suite of tests, that directly obtains the relevant $E_s$ for all possible types of analyses in every soil type. This is because the modulus varies considerably with strain level (or stress level). In certain geologic materials, it has in fact been possible to develop calibrated correlations between specific tests (e.g., PMT, DMT) with performance monitored data obtained from full-scale structures, including foundations and

embankments, or with reference values from laboratory test. These tests will provide a modulus somewhere along the stress-strain-strength curve (Fig. 2), generally at an intermediate level of strain. Of particular note, the small-strain modulus from shear wave velocity measurements provides an excellent reference value, as this is the maximum stiffness that the soil can exhibit at a given void ratio and effective confining state. Herein, a generalized approach based on the small strain stiffness from shear wave measurements will be discussed, whereby the initial modulus ($E_0$) is degraded to an appropriate stress level for the desired FOS.

The shear modulus degradation with shear strain is commonly shown in normalized form, with current G divided by the maximum $G_{max}$ (or $G_0$). The relationship between $G/G_0$ and logarithm of shear strain is well recognized for dynamic loading conditions (e.g., Vucetic and Dobry, 1991), however, the monotonic static loading shows a more severe decay with strain, as seen in Figure 3. The cyclic curve is representative of data obtained from resonant column tests, whereas the monotonic curve has been recently addressed by special internal & local strain measurements in triaxial tests, as well as by torsional shear devices (Jamiolkowski, et al. 1994).

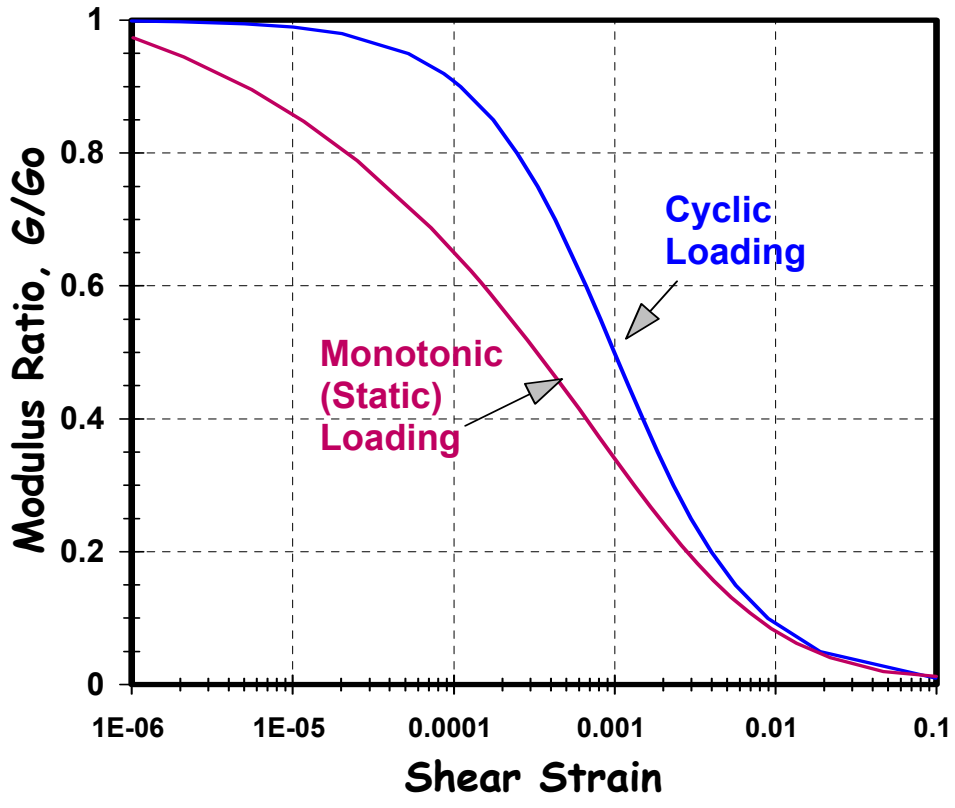


**Figure 3. Modulus Degradation with Log Shear Strain for Initial Monotonic (Static) and Dynamic (Cyclic) Loading Conditions.**

Laboratory monotonic shear tests with high-resolution deformation instrumentation have shown that strain data obtained external to the triaxial cells are flawed because of seating errors, bedding problems with the filter stone, and boundary effects at the specimen ends. New internal measurements are now possible that accurately measure the soil stiffness at small- to intermediate-strains (LoPresti, et al. 1993, 1995; Tatsuoka & Shibuya, 1992). Figure 4 shows a selection of normalized moduli ($E/E_0$) with varying stress level ($q/q_{ult}$) obtained on uncemented, unstructured geomaterials. Note here that an equivalent secant elastic modulus is used throughout.

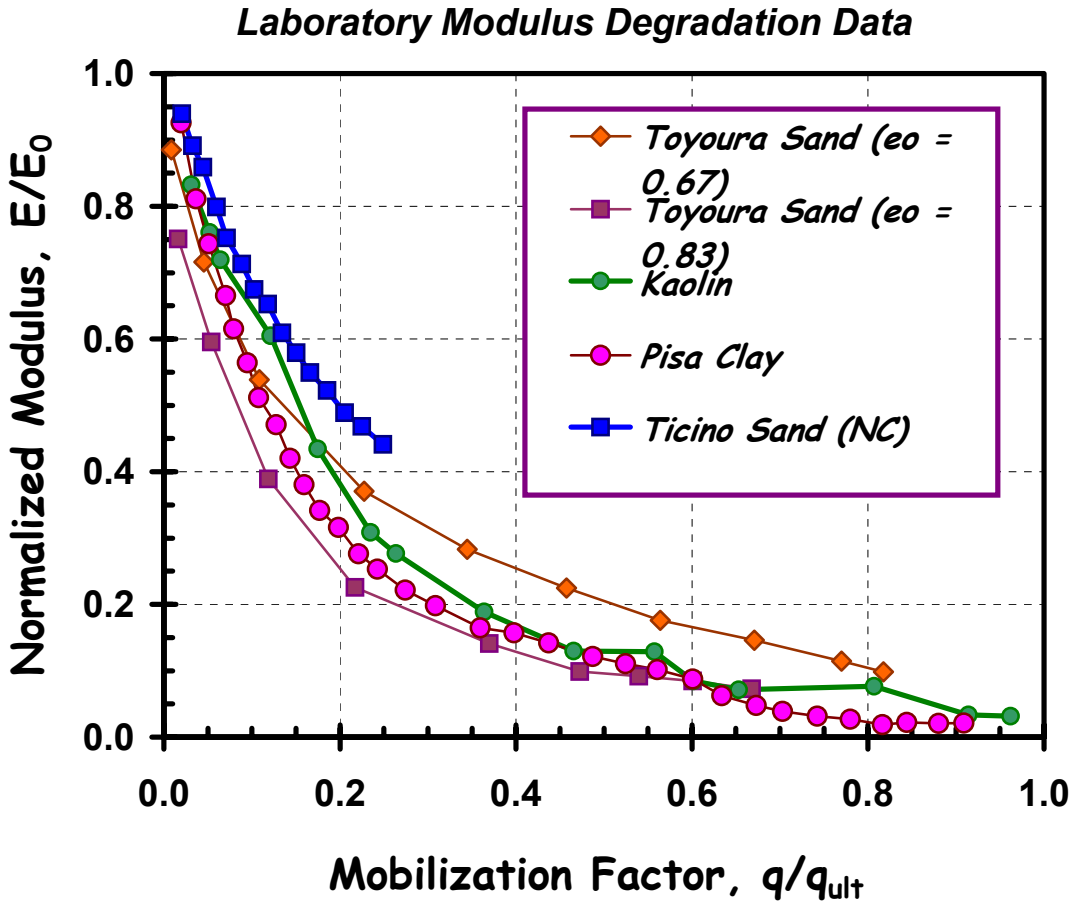


**Figure 4. Modulus Degradation from Instrumented Laboratory Tests on Uncemented and Unstructured Geomaterials.**

A modified hyperbola can be used as a simple means to reduce the small-strain stiffness ($E_0$) to secant values of E at working load levels, in terms of mobilized strength ($q/q_{ult}$). Figure 5 illustrates the suggested trends for unstructured clays and uncemented sands. The generalized form may be given as (Fahey & Carter, 1993):

$$E/E_0 = 1 - f\,(q/q_{ult})^g \qquad (1)$$

where *f* and *g* are fitting parameters. Values of *f* = 1 and *g* = 0.3 appear reasonable first-order estimates for unstructured and uncemented geomaterials (Mayne, et al. 1999a) and these provide a best fit for the data shown before in Figure 4. The mobilized stress level ($q/q_{ult}$) can also be considered as the reciprocal of the factor of safety (FS). That is, for ($q/q_{ult}$) = 0.5, the corresponding FS = 2.

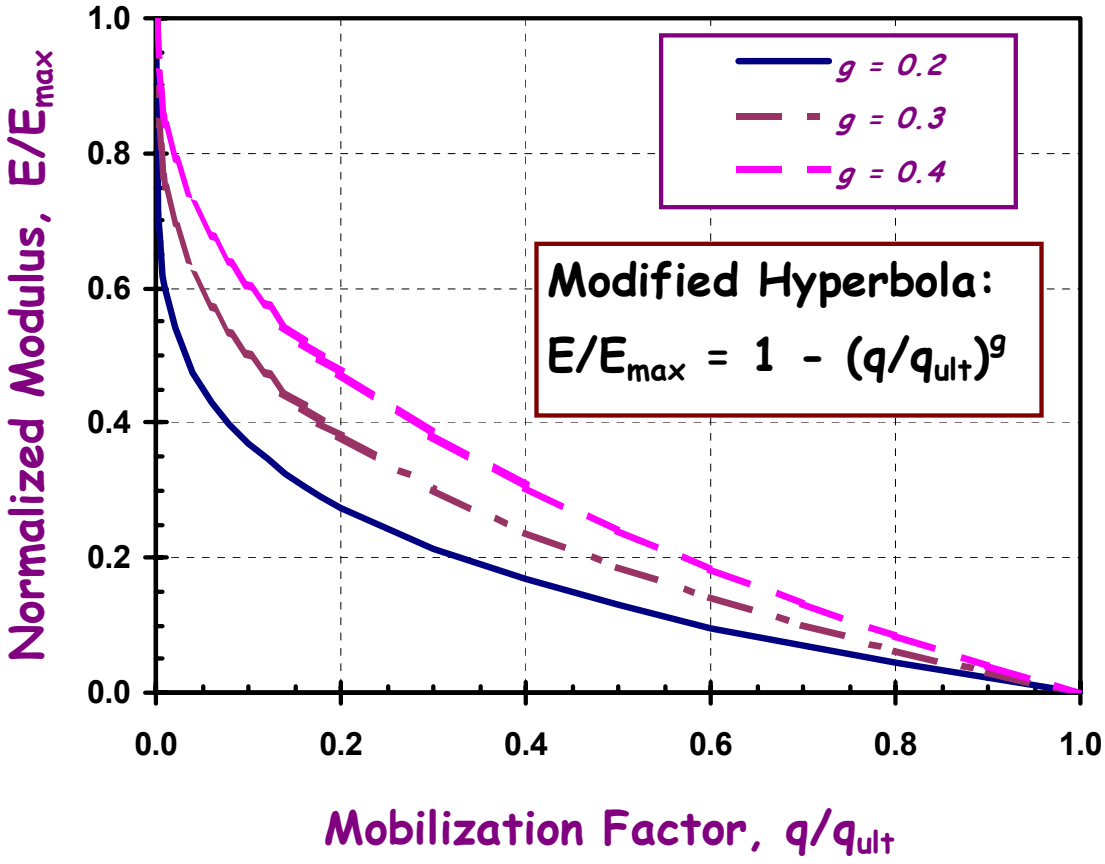


**Figure 5. Modified Hyperbolas with g= 0.2, 0.3, and 0.4 to Illustrate Modulus Degradation Curves. Note: Mobilized stress level $q/q_u$ = 1/FS.**

Other schemes for modulus degradation are available (e.g., Duncan & Chang, 1970; Hardin & Drnevich, 1972; Prevost & Keane, 1990; Tatsuoka & Shibuya, 1992). Several have a more fundamental basis or a better fitting over the full range of strains from small- to intermediate- to large-ranges (e.g., Puzrin & Burland, 1998). The intent here, however, is to adopt a simplified approach for facilitating the use of SCPTu data into foundation engineering analysis and for reducing the high initial stiffness as well as connecting small- and high-strain regions of soil response from shear wave and penetration data, respectively (Mayne & Dumas, 1997; Mayne, 1998).

## Evaluating Axial Displacements

The axial load-displacement behavior of deep foundations may be represented by elastic continuum theory where solutions have been developed from boundary element formulations (Poulos & Davis, 1980), finite elements (Poulos, 1989), and approximate closed-form analytical solutions (Randolph & Wroth, 1978, 1979; Fleming et al. 1985). Continuum theory characterizes the soil stiffness by two elastic parameters: an equivalent elastic soil modulus ($E_s$) and Poisson's ratio ($\nu_s$). Four generalized cases are considered: (1) homogeneous case where $E_s$ is constant with depth; and (2) a Gibson-type condition where $E_s$ is linearly-increasing with depth; (3) friction or floating-type piles; and (4) end-bearing type piles resting on a stiffer stratum. Figure 6 depicts the generalized stiffness profile for these cases, with corresponding definitions of moduli input for the analysis.

The vertical displacement ($w_t$) of a pile foundation subjected to axial compression loading is expressed (Poulos, 1987, 1989):

$$w_t = P_t I_\rho / (E_{sL} d) \qquad (2)$$

where $P_t$ = applied axial load at the top of the shaft, $E_{sL}$ = soil modulus along the sides

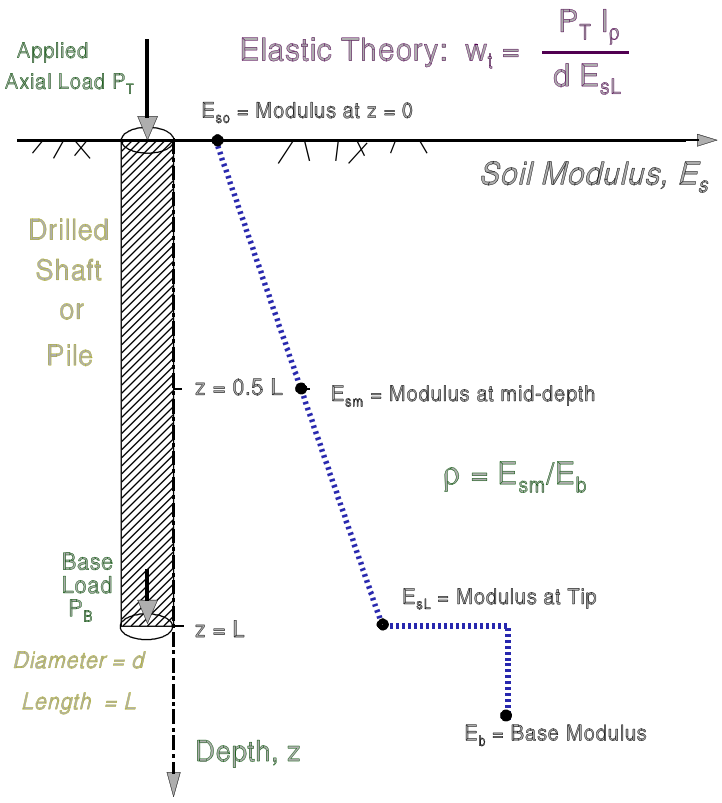

**Figure 6. Term Definitions Used in Elastic Continuum Model.**

at full depth (z = L), d = foundation diameter, and $I_\rho$ = displacement influence factor. The factor $I_\rho$ depends on the pile slenderness ratio (L/d), pile material, soil homogeneity, and relative soil-pile stiffness, as given in chart solutions, tables, or approximate closed-form. The latter is given in concise form (Randolph & Wroth, 1978, 1979; Poulos, 1987):

$$\mathbf{I_\rho} = 4(1+\nu) \frac{\left\{1 + \frac{1}{\pi\lambda} \frac{8}{(1-\nu_s)} \frac{\eta}{\xi} \frac{\tanh(\mu L)}{\mu L} \frac{L}{d}\right\}}{\left\{\frac{4}{(1-\nu_s)} \frac{\eta}{\xi} + \frac{4\pi\rho}{\varsigma} \frac{\tanh(\mu L)}{\mu L} \frac{L}{d}\right\}} \tag{3}$$

where the following terms apply:

d = shaft diameter.
L = pile length.
$\eta$ = $d_b/d$ = eta factor ($d_b$ = diameter of base, so that $\eta = 1$ for straight shafts).
$\xi$ = $E_{sL}/E_b$ = xi factor ($\xi = 1$ for floating pile; $\xi < 1$ for end-bearing).
$\rho^*$ = $E_{sm}/E_{sL}$ = rho ($\rho^* = 1$ for uniform soil; $\rho^* = 0.5$ for simple Gibson soil).
$\lambda$ = $2(1+\nu_s)E_p/E_{sL}$ = lambda factor.
$\varsigma$ = $\ln\{[0.25 + (2.5\rho^*(1-\nu_s) - 0.25)\xi] (2L/d)\}$ = zeta factor.
$\mu L$ = $2(2/\varsigma\lambda)^{0.5}$ (L/d) = mu factor.
$E_p$ = pile modulus (concrete plus reinforcing steel).
$E_{sL}$ = soil modulus value along pile shaft at level of base.
$E_{sm}$ = soil modulus value at mid-depth of pile shaft.
$E_b$ = soil modulus below foundation base (Note: $E_b = E_{sL}$ for floating pile).
$\nu_s$ = Poisson's ratio of soil.

Elastic continuum also provides an evaluation of axial load transfer distribution. The fraction of load transferred to the pile base ($P_b$) is given by (Fleming et al. 1985):

$$P_b/P_t = \frac{\left\{\frac{4}{(1-\nu_s)} \frac{\eta}{\xi} \frac{1}{\cosh(\mu L)}\right\}}{\left\{\frac{4}{(1-\nu_s)} \frac{\eta}{\xi} + \frac{4\pi\rho}{\varsigma} \frac{\tanh(\mu L)}{\mu L} \frac{L}{d}\right\}} \tag{4}$$

which conveniently has the same denominator as eq (3) for spreadsheet use. To account for the approximate nonlinear response, the modified hyperbola is used:

$$w_t = \frac{Q \cdot I_\rho}{d \cdot E_{max} \cdot [1 - f(Q/Q_{ult}]^g} \tag{5}$$

where Q = P = applied load and $Q_{ult} = P_{ult}$ = axial capacity for compression loading. Note

that the displacement influence factor also depends on current reduced $E_{sL}$.

**Axial Capacity Determinations**

The assessment of axial pile capacity ($Q_{ult} = Q_s + Q_b$) from CPT results is well-recognized (e.g., Robertson, et al. 1988; Poulos, 1989; Eslami & Fellenius, 1997). Of recent, Takesue, et al. (1998) offer a versatile direct CPT approach for side resistance of both drilled shafts and driven piles to obtain the pile side friction ($f_p$) in both clays and sands in terms of the measured $f_s$ and excess porewater pressures ($\Delta u_b$) during piezocone penetration. Using measurements with a porous filter located at the cone shoulder:

$$\text{For } \Delta u_b < 300 \text{ kPa: then } f_p = f_s \cdot [(\Delta u_b/1250) + 0.76] \quad (6a)$$

$$\text{For } \Delta u_b > 300 \text{ kPa: then } f_p = f_s \cdot [(\Delta u_b/200) - 0.50] \quad (6b)$$

In clays, the pile tip or pier base resistance ($q_b$) will be fully mobilized and can be evaluated from the effective cone resistance (Eslami & Fellenius, 1997):

$$\text{Clays: } q_b = q_t - u_b \quad (7)$$

In sands, however, full mobilization of the base develops fairly slowly, depending on the relative movement (s) with respect to pile width (B). Recent work by Lee & Salgado (1999) gives:

$$\text{Sands: } q_b \approx q_t \cdot [1.90 + \{0.62/(s/B)\}]^{-1} \quad (8)$$

**Coweta Shaft Load Test, Georgia**

The outlined procedure can be applied to a recent case study involving axial compression load testing of a drilled shaft for the widening and expansion of interstate I-85 in Coweta County, Georgia, located approximately 40 km south of Atlanta. The 0.91-m diameter shaft was constructed 19.2 m long under polymeric slurry to bear within the residuum and saprolite of the Piedmont geology. The base was situated in partially-weathered rock, as depicted in Figure 7. Results from standard penetration tests (SPT) in adjacent soil borings are also presented. The shaft was installed with an instrumented cage with 16 full-bridge electronic sister bars to measure load transfer with depth during applied axial loads.

The Piedmont Geologic Province is important in that many important cities and their expanding suburbs are located within its region, including Philadelphia, Baltimore, Washington-D.C., Richmond, Charlotte, Raleigh, and Atlanta. The current overburden consists of residual silty to sandy soils (ML to SM) that were derived from the in-place decomposition of the parent metamorphic and igneous rocks. These grade to saprolite and partially-weathered rock with depth (Sowers, 1994). Primary rock types include schist, gneiss, and granite, although localized regions include phyllite, slate, soapstone, greenstone, & diabase. The depth to parent rock varies locally because of differential weathering.

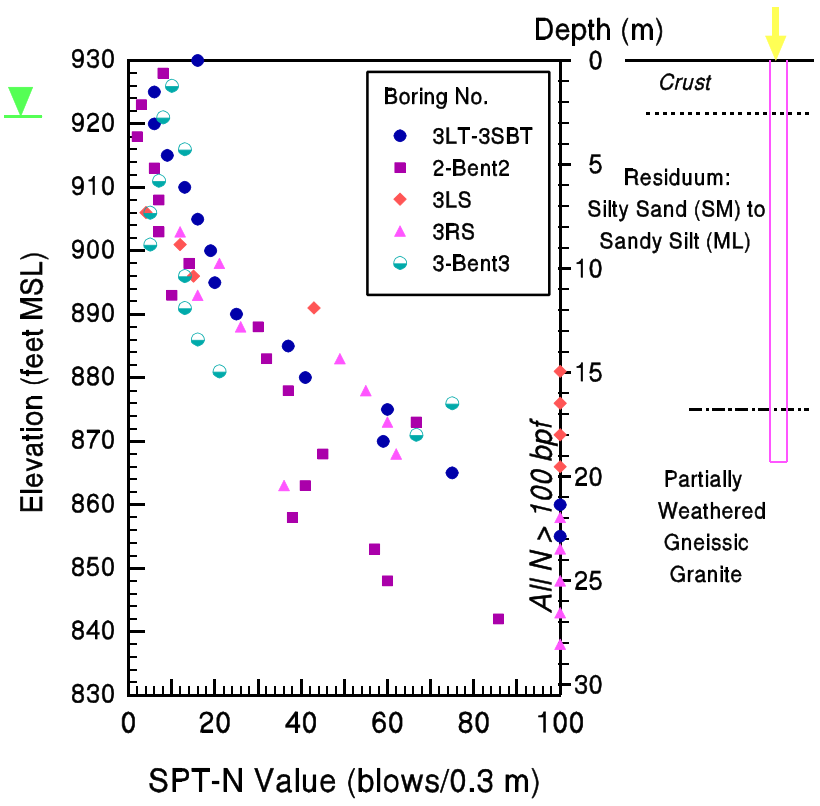


**Figure 7. SPT Summary and Drilled Shaft Profile at I-85 in Coweta County, GA.**

In the southern Piedmont, the overburden has been termed "Red Clay", based on common experiences with shallow topsoils affected by rainfall and their agricultural associations. In contrast, geotechnical categorization by the Unified Soils Classification System (USCS) place the residual materials as sandy silts (ML) and silty sands (SM). Thus, the opposite notions of clay versus sand have both been assigned to the Piedmont soils with respect to their behavior as either predominantly undrained or drained manner, as well in deciding which geotechnical tests are appropriate for defining the engineering parameters in analysis (Mayne, et al. 2000).

Two piezocones soundings were conducted at the site using a 10-cm$^2$ Hogentogler penetrometer with very similar results. One of these was a seismic piezocone test with the four independent readings, as presented in Figure 8 (sounding B). Both the tip stress ($q_t$) and sleeve friction ($f_s$) show a crustal zone extending to about 3 meters depth, underlain by firm residual silts and sands, with harder saprolite encountered below depths of 15 meters. An interesting facet of the Piedmont is the continuous negative porewater pressures at the shoulder element ($u_b$ or $u_2$) once the groundwater table is reached (Finke & Mayne, 1999). Here, the water table is located 2.8 m deep. In the vadoze zone above, porewater pressures can be positive, zero, or negative, depending upon the degree of saturation and ambient capillarity. Generally, full dissipation occurred to hydrostatic within 1 to 3 minutes. The downhole measurement of shear wave velocity ($V_s$) also confirmed a crust and increase of stiffness with depth in the natural residuum.

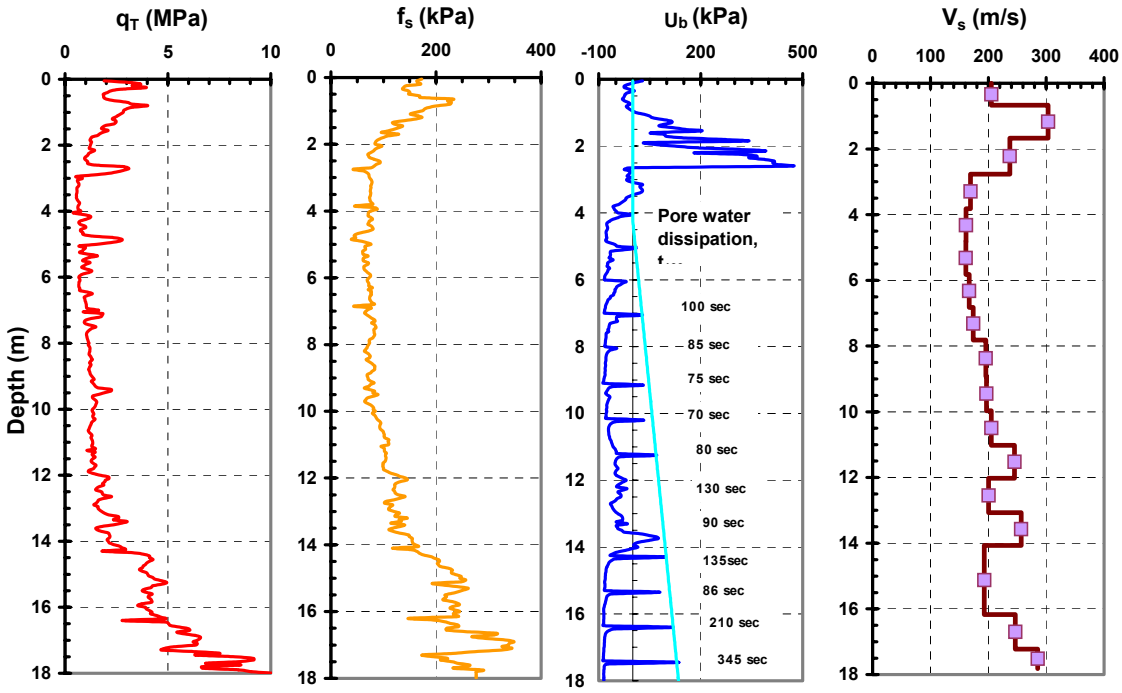


**Figure 8. Results of Seismic Piezocone Sounding at Coweta Bridge Site.**

A maximum tip stress of 32 MPa was recorded in the partially-weathered rock during sounding A. Assuming a maximum mobilized movement at the base of (s/B) = 10%, equation (8) gives a reduction factor ($q_b/q_t$) = 0.123, or unit base resistance of $q_b$ = 3.95 MPa. For the base area $A_b$ = 0.65 m$^2$, an end bearing component of $Q_b$ = 2.56 MN is calculated. For each depth reading at 50-mm intervals, the unit side friction was calculated based on the $\Delta u_b$ readings, giving an average $f_p/f_s$ ratio = 0.71, and overall pile side resistance of $f_p$ = 87 kPa per equation (6). For the total surface area of $A_s$ = 55 m$^2$, the calculated total side capacity is $Q_s$ = 4.78 MN. Thus, the total capacity of the shaft is evaluated as $Q_t = Q_s + Q_b$ = 7.24 MN from the CPT data.

The shear wave data are processed to obtain the initial stiffness using the following relationship for saturated soil mass density (Mayne, et al., 1999a).

$$\rho_{sat} \approx 1 + \frac{1}{0.614 + 58.7(logz + 1.095)/V_s} \qquad (9)$$

where $\rho_{sat}$ is in g/cc, depth z is in meters, and $V_s$ in m/s. Note that dry density (and dry unit weights) can be evaluated from the saturated value from:

$$\rho_{dry} = \frac{G_s(\rho_{sat} - 1)}{G_s - 1} \tag{10}$$

In the vadose zone with partial saturation, the total unit weight would fall between these two extremes. The derived parameters of mass density and initial elastic modulus with depth are presented in Figure 9.

It can be seen that the stiffness increases approximately linearly with depth, as represented by a Gibson-type soil. Previous results in the Piedmont geology from spectral analysis of surface waves (SASW) conducted at the Georgia Tech campus have given similar results to these downhole values (Mayne & Dumas, 1997).

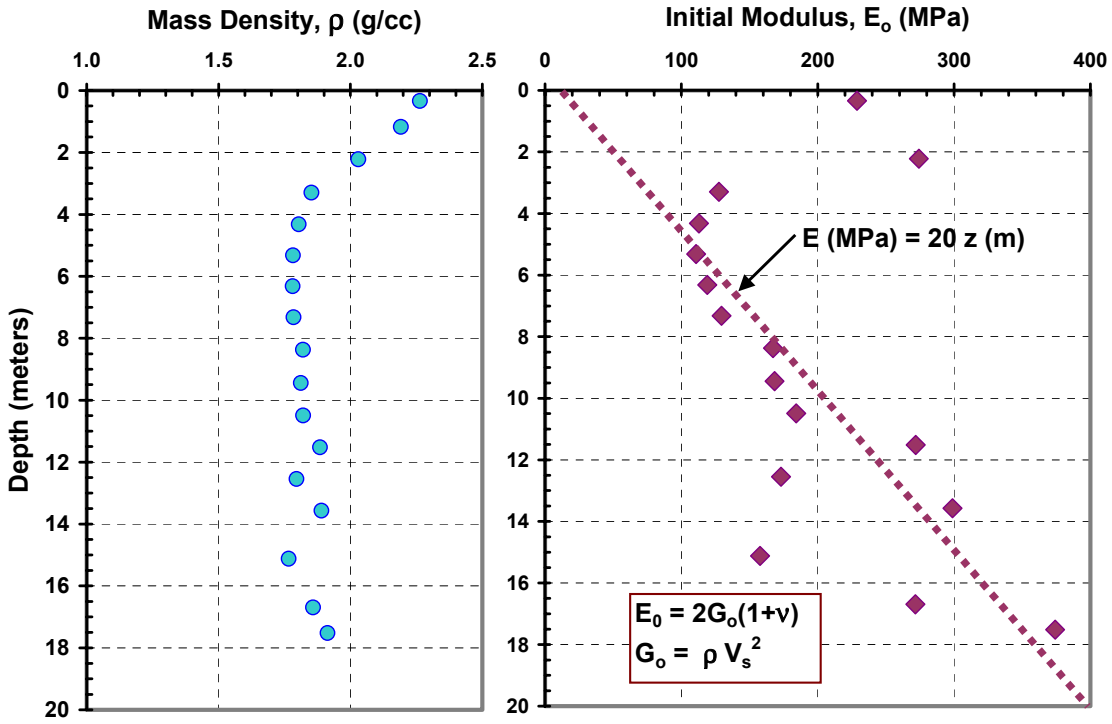


**Figure 9. Derived Profiles of Density and Small-Strain Elastic Modulus at I-85.**

For the elastic continuum analysis of displacements, the initial soil modulus along the shaft at the full length (z = L) is taken as $E_{sL}$ = 360 MPa, giving the modulus rho term $\rho^* = E_{sm}/E_{sL} = 0.5$ for this site. The xi ratio is based on previous studies of end-bearing deep foundations in the Piedmont (Mayne, et al. 1999b) and taken as $\xi = 0.25$, or ratio $E_{sL}/E_b = 4$, although $E_{sL}/E_b$ ratios of 1 to10 still provide reasonable predictions herein. A pile material modulus of $E_p$ = 27.8 GPa is used for the drilled shaft.

The full predictions of total load, shaft load, and base load versus deflection at the top of the shaft are presented in Figure 10 in comparison with the measured axial loads and displacements. Also shown are the load transfer measurements to the base derived from the instrumented reinforcing cage. The nonlinear simulation is seen to well represent the nonlinear load-deflection response throughout the full testing range from 0 to 45 mm. In addition, the elastic continuum theory correctly proportions the amount of load distribution amongst the side and base components. For the final loading condition at 45 mm deflection, 72% of the total compression load is taken in side shear and 28% transfer to the base.

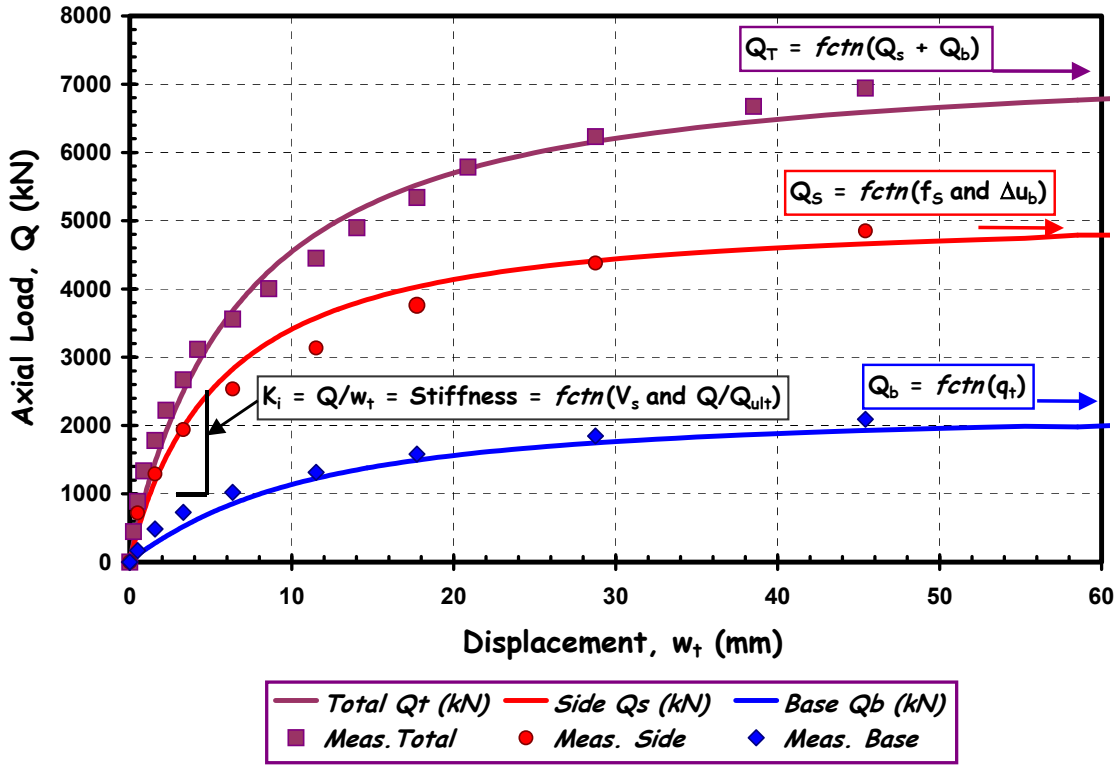


**Figure 10. Measured and Predicted Load-Displacement and Load Transfer Response of Drilled Shaft at I-85 Load Test.**

## Conclusions

The in-situ shear wave velocity provides a fundamental reference stiffness for the evaluation of foundation systems. An elastic continuum formulation can be used to represent the axial load-displacement response and proportion of load transfer in side and base. A modulus degradation scheme is used to approximate nonlinear effects. Results of seismic piezocone tests are useful in providing data for both capacity calculations and small-strain stiffness from a single sounding.

**Acknowledgments**

The authors acknowledge the funding support received from the National Science Foundation (NSF) and International Association of Foundation Drilling (ADSC). Thanks to Tom Scruggs of the Georgia DOT in gaining access to the Coweta site and to Professor Mike O'Neill of the University of Houston in conducting and sharing the results of the load test. Tom Casey and Alec McGillivray performed the SCPTu soundings.

**References**

Burland, J.B. (1989). Small is beautiful: The stiffness of soils at small strains. *Canadian Geotechnical Journal* 26 (4), 499-516.

Burns, S.E. and Mayne, P.W. (1996). Small- and high-strain soil properties using the seismic piezocone. *Transportation Research Record* 1548, National Academy Press, Washington, D.C., 81-88.

Duncan, J.M. and Chang, C.Y. (1970). Nonlinear analysis of stress and strains in soils. *Journal of the Soil Mechanics & Foundations Div.* (ASCE) 96 (SM5), 1629-1653.

Eslami, A. and Fellenius, B.H. (1997). Pile capacity by direct CPT and CPTu methods applied to 102 cas histories. *Canadian Geotechnical Journal* 34 (6), 886-904.

Fahey, M. and Carter, J. (1993). A finite element study of the pressuremeter using a nonlinear elastic plastic model. *Canadian Geotechnical Journal* 30 (2), 348-362.

Finke, K.A., Mayne, P.W. and Klopp, R.A. (1999). Characteristic piezocone response in Piedmont residual soils. *Behavioral Characteristics of Residual Soils*. GSP No. 92, ASCE, Reston/VA, 1-11.

Fleming, W.G.K., Weltman, A.J., Randolph, M.F., and Elson, W.K. (1985). *Piling Engineering*, Surrey University Press, Wiley & Sons, New York, 380 p.

Hardin, B.O. and Drnevich, V.P. (1972). Shear modulus and damping in soils. *Journal of the Soil Mechanics & Foundations Div.* (ASCE) 98 (7), 667-692.

Jamiolkowski, M., Lancellotta, R., LoPresti, D.C.F. and Pallara. O. (1994). Stiffness of Toyoura sand at small and intermediate strain, *Proceedings, 13th International Conference on Soil Mechanics & Foundation Engineering* (3), New Delhi, 169-173.

Lee, J.H. and Salgado, R. (1999). Determination of pile base resistance in sands. *Journal of Geotechnical & Geoenvironmental Engineering* 125 (8), 673-683.

LoPresti, D.C.F., Pallara, O., Lancellotta, R., Armandi, M., and Maniscalco, R. (1993). Monotonic and cyclic loading behavior of two sands at small strains, ASTM *Geotechnical Testing Journal* 16 (4), 409-424.

LoPresti, D.C.F., Pallara, O. and Puci, I. (1995). A modified commercial triaxial testing system for small-strain measurements. ASTM *Geotechnical Testing Journal* 18 (1), 15-31.

Mayne, P.W, and Dumas, C. (1997). Enhanced in-situ geotechnical testing for bridge foundation analyses. *Transportation Research Record 1569*, National Academy Press, Washington, D.C., 26-35.

Mayne, P.W. (1998). Site characterization aspects of Piedmont residual soils in eastern United States. *Proceedings*, 14th International Conference on Soil Mechanics & Foundation Engineering, Vol. 4, Hamburg; Balkema, Rotterdam, 2191-2195.

Mayne, P.W., Schneider, J.A., and Martin, G.K. (1999a). Small- and large-strain soil

properties from seismic flat plate dilatometer tests. *Pre-Failure Deformation Characteristics of Geomaterials*, Vol. 1, (Torino), Balkema, Rotterdam, 419-426.

Mayne, P.W., Martin, G.K., and Schneider, J.A. (1999b). Flat dilatometer modulus applied to drilled shafts in the Piedmont residuum. *Behavioral Characteristics of Residual Soils*. GSP No. 92, ASCE, Reston/VA, 101-112.

Mayne, P.W., Brown, D.A., Vinson, J., Schneider, J.A. and Finke, K.A. (2000). Site characterization of Piedmont residual soils at the NGES, Opelika, AL. National Geotechnical Experimentation Sites, GSP No. 93, ASCE, Reston, VA, 160-185.

O'Neill, M.W. and Reese, L.C. (1999). *Drilled Shafts: Construction Procedures & Design Methods*, Volumes I & II, Publication No. FHWA-IF-99-025, U.S. Dept. of Transportation, published by ADSC, Dallas, 758 p.

Poulos, H.G. and Davis, E.H. (1980), *Pile Foundation Analysis and Design*, Wiley & Sons, New York, 397 p. (reprinted by Krieger Publishing, Florida, 1990).

Poulos, H.G. (1987). From theory to practice in pile design (E.H. Davis Memorial Lecture). *Transactions*, Australian Geomechanics Society, Sydney, 1-31.

Poulos, H.G. (1989). Pile behavior: theory and application", 29th Rankine Lecture, *Geotechnique*, Vol. 39, No. 3, September, 363-416.

Prevost, J.H. and Keane, C.M. (1990). Shear stress-strain curve generation form simple material parameters. *Journal of Geotechnical Engineering* 116 (8), 1255-1263.

Puzrin, A.M. and Burland, J.B. (1998). Nonlinear model of small-strain behavior of soils. *Geotechnique* 46 (1), 157-164.

Randolph, M.F. and Wroth, C.P. (1978). Analysis of deformation of vertically loaded piles. *Journal of the Geotechnical Engineering Division*, ASCE, Vol. 104 (GT12), 1465-1488.

Randolph, M.F. and Wroth, C.P. (1979). A simple approach to pile design and the evaluation of pile tests. *Behavior of Deep Foundations*, STP 670, ASTM, 484-499.

Robertson, P.K., Campanella, R.G., Davies, M.P. and Sy, A. (1988). Axial capacity of driven piles in deltaic soils using CPT. Penetration Testing 1988 (2), Balkema, Rotterdam, 919-928.

Sowers, G.F. (1994). Residual soil settlement related to the weathering profile. *Vertical and Horizontal Deformations of Foundations & Embankments*, Vol. 2, (GSP No. 40), ASCE, New York, 1689-1702.

Takesue, K., Sasao, H., and Matsumoto, T. (1998). Correlation between ultimate pile skin friction and CPT data. *Geotechnical Site Characterization* (2), Balkema, Rotterdam, 1177-1182.

Tatsuoka, F. and Shibuya, S. (1992). Deformation characteristics of soils and rocks from field and laboratory tests. *Report of the Institute of Industrial Science*, Vol. 37, No. 1, Serial No. 235, The University of Tokyo, 136 p.

Vucetic, M. and Dobry, R. (1991). Effect of soil plasticity on cyclic response. *Journal of Geotechnical Engineering* 117 (1), 89-107.